J. At. Mol. Sci.
doi: 10.4208/jams.011811.022011a

Vol. **2**, No. 3, pp. 187-202
August 2011

Study of coherent π^0–photoproduction on the deuteron

E. M. Darwish[a,b,*], N. Akopov[c], and M. A. El-Zohry[d]

[a] *Applied Physics Department, Faculty of Applied Science, Taibah University, P. O. Box 1343, Al-Madinah Al-Munawarah, Saudi Arabia*
[b] *Physics Department, Faculty of Science, Sohag University, Sohag 82524, Egypt*
[c] *Yerevan Physics Institute, Br. Alikhanian 2, 0036 Yerevan, Armenia*
[d] *Yerevan State University, A. Manoogian 1, 0025 Yerevan, Armenia*

Received 18 January 2011; Accepted (in revised version) 20 Feburary 2011
Published Online 28 March 2011

Abstract. We consider the coherent π^0–photoproduction reaction on the deuteron, $\gamma d \to \pi^0 d$, in the energy region from π-threshold up to 1 GeV using an enhanced elementary pion photoproduction amplitude on the free nucleon and a realistic high-precision NN potential model for the deuteron wave function. Numerical results for total and differential cross sections are presented for which the sensitivity to various models for the elementary pion photoproduction operator is investigated. Considerable dependence of the results on the elementary amplitude is found at photon lab-energies close to π-threshold and above 600 MeV. In addition, the results for differential and total cross sections are compared with the available experimental data and a satisfactory agreement was found.

PACS: 13.60.Le, 25.20.Lj, 14.20.Gk

Key words: Meson production, photoproduction reactions, Baryon resonances

1 Introduction

The study of pion production processes on the deuteron are of fundamental interest in nuclear physics. The photoproduction of mesons is an excellent tool for the study of nucleon resonances [1] and in consequence of the structure of the nucleon. In this context, meson production on the deuteron is of specific importance due to the lack of free neutron targets. With respect to pion production, both possible reactions, the coherent and the incoherent one, are worth to be studied. Coherent pion photoproduction on the deuteron may be used as an isospin filter and is especially sensitive to the coherent sum of the $\gamma p \to \pi^0 p$ and $\gamma n \to \pi^0 n$ amplitude. On the other hand, incoherent pion photoproduction on the deuteron may be used

*Corresponding author. *Email address:* `eeddarwish@yahoo.com` (E. M. Darwish)

to obtain information about neutron cross section in quasi-free kinematics. Due to its relative simplicity, the deuteron is the ideal target for such studies.

Most recently, an improved calculation of the incoherent pion photoproduction on the deuteron has been performed in Ref. [2] in which final-state interactions (FSI) are included completely in the NN- and πN-subsystems and an enhanced elementary pion photoproduction operator taken from Ref. [3] has been used. The influence of the elementary operator on cross sections and spin observables for both the neutral and the charged pion production channels has been investigated and was found to be very important. In many cases the deviation among results obtained using different operators is very large.

For a long time, coherent π^0-photoproduction on the deuteron has been studied as a source of information on the elementary π^0-photoproduction off the neutron. This reaction has been first studied by Koch and Woloshyn [4] by including the contribution from pion rescattering with charge exchange contributions. This effect was then verified by Bosted and Laget [5] in studies of coherent π^0-photoproduction from the deuteron in the threshold region. In Ref. [6] an approach of $NN-N\Delta$ coupled channels for describing coherent π^0-photoproduction from the deuteron in the $\Delta(1232)$-resonance region was used. In another approach, developed in Ref. [7], relativistic Feynman diagrams have been evaluated. Blaazer *et al.* [8] studied rescattering corrections to all orders by solving Faddeev equations of the πNN-system. They have concluded that the contributions of the neutron and the proton cannot be separated because of the charge-exchange rescattering of the pion. Using a microscopic approach based on the Kerman-McManus-Thaler (KMT) multiple scattering theory [9] in momentum space, Kamalov *et al.* [10] have studied coherent π^0-photoproduction from the deuteron in the $\Delta(1232)$-resonance region in a coupled channel approach.

The coherent π^0-photoproduction from the deuteron was studied by Kudryavtsev *et al.* [11]. In particular, it was demonstrated that at large c.m. angles and photon lab-energies between 600 and 800 MeV, the two-step process with the excitation of an intermediate η-meson dominates over single-step process photoproduction and pion rescattering. The main conclusion of Ref. [11] were reproduced in another paper [12], where it was shown that in addition to this two-step process, the full dynamics in the intermediate $NN\eta$ system could be important as well. Unfortunately, none of these theoretical studies considers the energy region above the $\Delta(1232)$-resonance region and/or investigates the sensitivity to the elementary pion photoproduction operator on the free nucleon. Therefore, the coherent π^0-photoproduction reaction on the deuteron has been investigated in the $\Delta(1232)$-resonance region Ref. [13] with special emphasize on the doubly polarized cross sections. The sensitivity of the results to the elementary pion photoproduction amplitude was investigated, and considerable dependence has been found.

Our purpose in the present paper is, therefore, to extend the model, recently presented in [13], to make theoretical predictions for unpolarized total and differential cross sections of the process $\gamma d \to \pi^0 d$ in the energy range from π-threshold up to 1 GeV. For the elementary $\gamma N \to \pi N$ amplitude, an enhanced elementary pion photoproduction operator taken from Ref. [3] is used. This model displays chiral symmetry, gauge invariance, and crossing symmetry, as well as a consistent treatment of the interaction with spin-3/2 particles. It also provides a reliable description of the threshold region. For the deuteron wave function, we used the realistic high-precision CD-Bonn potential model [14]. The calculation of this work is of theoretical interest because it provides an important test of our understanding of the elementary neutron amplitude in the absence of a neutron target.

This paper is organized as follows. In Section 2, a brief review of the formalism for the reaction $\gamma d \to \pi^0 d$, in which the transition matrix elements are calculated, is given. Results for unpolarized total and differential cross sections are presented and discussed in Section 3, focusing on the sensitivity of results to the elementary pion photoproduction operator. Finally, we provide conclusions in Section 4. Throughout the paper we use natural units $\hbar = c = 1$.

2 Formalism

As a starting point, we will first consider the formalism for coherent π^0-photoproduction on the deuteron which contains only two particles in the initial and in the final states. The general form of the two-body reaction is

$$a(p_a) + b(p_b) \longrightarrow c(p_c) + d(p_d), \tag{1}$$

where $p_i = (E_i, \vec{p}_i)$ denotes the four-momentum of particle "i" with $i \in \{a,b,c,d\}$.

Following the conventions of Bjorken and Drell [15], the general form for the differential cross section of a two-particle reaction in the center-of-mass (c.m.) system is given by

$$\frac{d\sigma}{d\Omega_c} = \frac{1}{(2\pi W)^2} \frac{p_c}{p_a} \frac{E_a E_b E_c E_d}{F_a F_b F_c F_d} \frac{1}{s} \sum_{\mu_d \mu_c \mu_b \mu_a} \left| T_{\mu_d \mu_c \mu_b \mu_a}(\vec{p}_d, \vec{p}_c, \vec{p}_b, \vec{p}_a) \right|^2 \tag{2}$$

with $T_{\mu_d \mu_c \mu_b \mu_a}$ as reaction matrix, μ_i denoting the spin projection of particle "i" on some quantization axis, and F_i is a factor arising from the covariant normalization of the states and its form depends on whether the particle is a boson ($F_i = 2E_i$) or a fermion ($F_i = E_i/m_i$), where E_i and m_i are its energy and mass, respectively. The factor $s = (2s_a+1)(2s_b+1)$ takes into account the averaging over the initial spin states, where s_a and s_b denote the spins of the incoming particles a and b, respectively. All momenta are functions of the invariant mass of the two-body system W, i.e. $p_i = p_i(W)$, where $W = E_a + E_b = E_c + E_d$.

Focusing on coherent π^0-photoproduction from the deuteron and choosing the photon-deuteron c.m. frame with the z-axis along the photon momentum $\vec{k}$, the y-axis parallel to $\vec{k} \times \vec{q}$ and the x-axis such as to form a right-handed system. Thus the outgoing pion is described by the spherical angles ϕ_{π^0} and θ_{π^0} with $\cos\theta_{\pi^0} = \hat{q} \cdot \hat{k}$. The reaction (1) then becomes

$$\gamma(E_\gamma, \vec{k}, \lambda) + d(E_d, -\vec{k}) \longrightarrow \pi^0(E_{\pi^0}, \vec{q}) + d(E'_d, -\vec{q}), \tag{3}$$

where energy and momenta of the participating particles are given in the parentheses, and λ stands for the circular photon polarization. Diagrammatic representation of this reaction is shown in Fig. 1. The F_i factor is given by

$$F_a = 2E_\gamma, \qquad F_b = 2E_d, \qquad F_c = 2E_{\pi^0}, \qquad F_d = 2E'_d, \tag{4}$$

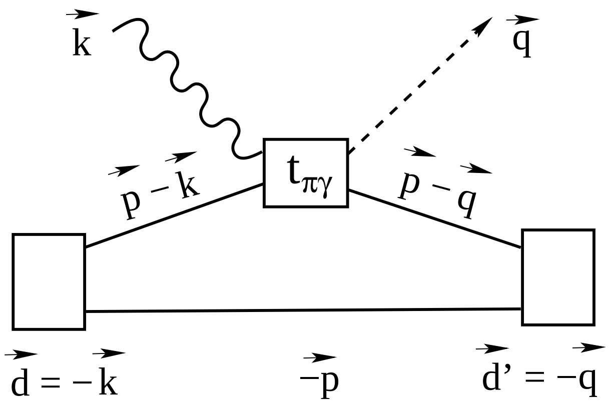

Figure 1: Diagrammatic representation of the $\gamma d \to \pi^0 d$ reaction in the impulse approximation with definition of momenta in the γd c.m. system.

and therefore one finds $s=6$ taking into account the averaging of the cross section over the initial two possible polarizations of the real photon and the three spin projections of the deuteron.

Using standard normalization of particle states, the unpolarized differential cross section of the reaction $\gamma d \to \pi^0 d$ in the c.m. system is then given by

$$\frac{d\sigma}{d\Omega_{\pi^0}} = \frac{E_d E_d'}{(4\pi W_{\gamma d})^2} \frac{|\vec{q}|}{|\vec{k}|} \frac{1}{6} \sum_{m_d m_d' \lambda} \left| T_{m_d m_d' \lambda}(\vec{k},\vec{q}) \right|^2, \tag{5}$$

where m_d' (m_d) is the spin projection of the outgoing (incoming) deuteron and $\vec{q}$ and $\vec{k}$ are the c.m. momenta of the pion and photon, respectively. Moreover, the invariant energy of the γd system is given as

$$\begin{aligned} W_{\gamma d} &= E_\gamma + \sqrt{\vec{k}^2 + M_d^2}, \qquad E_\gamma = |\vec{k}|, \\ &= E_{\pi^0} + \sqrt{\vec{q}^2 + M_d^2}, \qquad E_{\pi^0} = \sqrt{\vec{q}^2 + m_{\pi^0}^2}, \end{aligned} \tag{6}$$

where M_d and m_{π^0} are the deuteron and neutral-pion masses, respectively.

The scattering amplitude of coherent π^0-photoproduction on the deuteron is given in the impulse approximation by

$$T_{m_d m_d' \lambda}(\vec{k},\vec{q}) = 2 \int \frac{d^3 p}{(2\pi)^3} \, \phi_{m_d'}^{\dagger}(\vec{p}\,') \, t_{\gamma\pi}^{\lambda}(\vec{k},\vec{p}_i,\vec{q},\vec{p}_f) \, \phi_{m_d}(\vec{p}) \tag{7}$$

with $t_{\gamma\pi}^{\lambda}$ standing for the corresponding elementary amplitude $\gamma N \to \pi N$. Furthermore, the vectors $\vec{p}_i$ and $\vec{p}_f$ denote initial and final momenta of the active nucleon in the deuteron, for which we have $\vec{p}_i = \vec{p} - \vec{k}/2$ and $\vec{p}_f = \vec{p} - \vec{q} + \vec{k}/2$, and $\vec{p}\,' = \vec{p} + (\vec{k} - \vec{q})/2$ denotes the relative momentum in the final deuteron state. The time-ordered diagrams taken into account in the present work for the scattering amplitude of coherent π^0-photoproduction on the deuteron are depicted in Fig. 2. As the neutral pion has neither charge nor spin, the photon cannot couple to its charge and magnetic moment. So, the mechanisms embodied in diagrams (c), (d), and (e) in Fig. 2 and the corresponding ones in Fig. 3 for charged pions do contribute to neutral-pion production, but only in the intermediate state, where first a charged particle is produced, that turns into a neutral one upon rescattering.

Introducing a partial wave decomposition, one finds for the scattering matrix the relation

$$T_{m_d m'_d \lambda}(\vec{k},\vec{q}) = e^{i(m_d+\lambda)\phi_{\pi^0}}\, t_{m_d m'_d \lambda}(W_{\gamma d},\theta_{\pi^0}), \tag{8}$$

where the reduced t-matrix elements are the basic quantities that determine cross sections and polarization observables. If parity is conserved, the reduced t-matrix obeys the symmetry relation

$$t_{-m_d -m'_d -\lambda} = (-)^{1+m_d+m'_d+\lambda}\, t_{m_d m'_d \lambda}. \tag{9}$$

For the deuteron wave function we use the familiar ansatz

$$\phi_{m_d}(\vec{p}) = \sum_{L=0,2} \sum_{m_L m_S} (L m_L 1 m_S | 1 m_d)\, u_L(p)\, Y_{L m_L}(\hat{p})\, \chi_{m_S} \zeta_0, \tag{10}$$

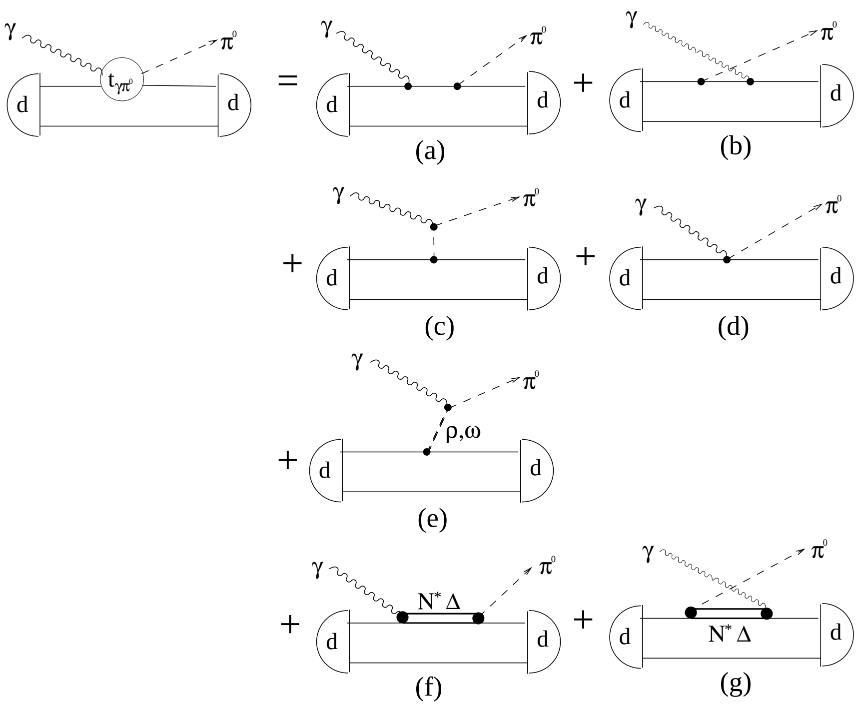

Figure 2: The considered diagrams in coherent pion photoproduction on the deuteron. Born terms: (a) direct nucleon pole, (b) crossed nucleon pole, (c) pion pole, and (d) Kroll-Rudermann contact term; (e) vector-meson exchange (ρ and ω); resonance excitations contribution: (f) direct and (g) crossed.

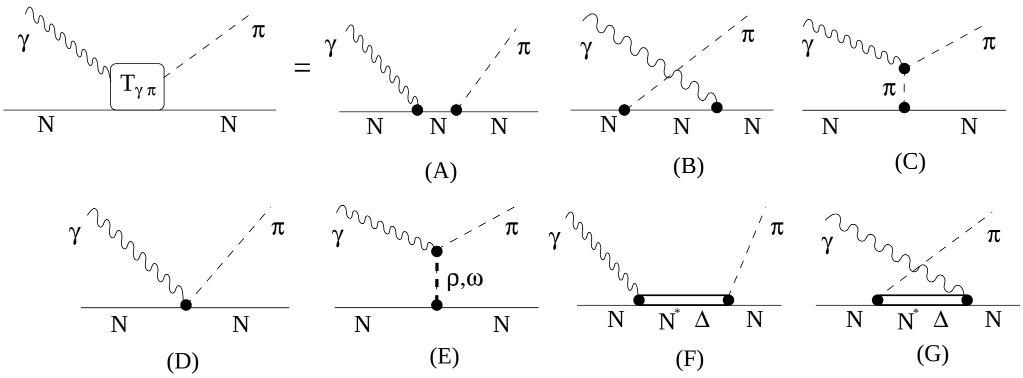

Figure 3: Feynman diagrams for pion photoproduction from a single nucleon. Born terms: (A) direct nucleon pole, (B) crossed nucleon pole, (C) pion in flight, and (D) Kroll-Rudermann contact term; (E) vector-meson exchange (ρ and ω); resonance excitations contribution: (F) direct and (G) crossed.

where the last two terms denote spin and isospin wave functions, respectively. In the present work, the radial deuteron wave functions of the initial and final deuteron state are chosen to be identical for consistency, i.e., both from the realistic high-precision CD-Bonn potential model [14].

For the elementary pion photoproduction operator on the free nucleon, $\gamma N \to \pi N$, we use in this work the effective Lagrangian approach (ELA) elaborated in Ref. [3], which has been applied successfully from threshold up to 1 GeV of photon energy in the laboratory reference system and succeeds to reconcile [16] pion photoproduction experiments in the $\Delta(1232)$ region [17, 18] with the latest Lattice QCD calculations of the quadrupole deformation of the $\Delta(1232)$ [19]. Recently, the model has also been applied successfully to eta photoproduction from the proton [20]. This model is based upon an effective Lagrangian approach which from a theoretical point of view is a very appealing, reliable, and formally well-established approach in the energy region of the mass of the nucleon. It displays chiral symmetry, gauge invariance, and crossing symmetry as well as a consistent treatment of the spin-3/2 interaction. The model includes Born terms (diagrams (A)-(D) in Fig. 3), vector-meson exchanges (ρ and ω, diagram (E) in Fig. 3), and all the four star resonances in Particle Data Group (PDG) [17] up to 1.7 GeV and up to spin-3/2: $\Delta(1232)$, N(1440), N(1520), $\Delta(1620)$, N(1650), and $\Delta(1700)$ (diagrams (F) and (G) in Fig. 3). Born terms are calculated using the Lagrangian

$$\begin{aligned}\mathscr{L}_{Born} = & -ieF_1^V \hat{A}^\alpha \epsilon_{jk3} \pi_j (\partial_\alpha \pi_k) - e\hat{A}^\alpha F_1^V \bar{N} \gamma_\alpha \frac{1}{2}\left(F_1^{S/V} + \tau_3\right) N \\ & -ieF_1^V \frac{f_{\pi N}}{m_\pi} \hat{A}^\alpha \bar{N} \gamma_\alpha \gamma_5 \frac{1}{2}[\tau_j, \tau_3] \pi_j N - \frac{ie}{4M_N} F_2^V \bar{N} \frac{1}{2}\left(F_2^{S/V} + \tau_3\right) \gamma_{\alpha\beta} N F^{\alpha\beta} \\ & + \frac{f_{\pi N}}{m_\pi} \bar{N} \gamma_\alpha \gamma_5 \tau_j N \left(\partial^\alpha \pi_j\right), \end{aligned} \tag{11}$$

where e is the absolute value of the electron charge, m_π the mass of the pion, M_N the mass of the nucleon, $f_{\pi N}$ the pion nucleon coupling constant, $F_j^V = F_j^p - F_j^n$ and $F_j^S = F_j^p + F_j^n$ are the isovector and isoscalar nucleon form factors, $F^{\mu\nu} = \partial^\mu \hat{A}^\nu - \partial^\nu \hat{A}^\mu$ is the electromagnetic field ($\hat{A}^\mu$ stands for the photon field), N the nucleon field, and π_j the pion field. The coupling to the pion has been chosen pseudovector in order to ensure the correct parity and low energy behavior.

The main contribution of mesons to pion photoproduction is given by ρ (isospin-1 spin-1) and ω (isospin-0 spin-1) exchange. The phenomenological Lagrangians which describe vector mesons are:

$$\begin{aligned}
\mathscr{L}_\omega &= -F_{\omega NN}\bar{N}\left[\gamma_\alpha - i\frac{K_\omega}{2M_N}\gamma_{\alpha\beta}\partial^\beta\right]\omega^\alpha N + \frac{eG_{\omega\pi\gamma}}{2m_\pi}\epsilon_{\mu\nu\alpha\beta}F^{\alpha\beta}\left(\partial^\mu\pi_j\right)\delta_{j3}\omega^\nu, \\
\mathscr{L}_\rho &= -F_{\rho NN}\bar{N}\left[\gamma_\alpha - i\frac{K_\rho}{2M_N}\gamma_{\alpha\beta}\partial^\beta\right]\tau_j\rho_j^\alpha N + \frac{eG_{\rho\pi\gamma}}{2m_\pi}\epsilon_{\mu\nu\alpha\beta}F^{\alpha\beta}\left(\partial^\mu\pi_j\right)\rho_j^\nu. \qquad (12)
\end{aligned}$$

As already mentioned above, these terms are absent in the case of direct neutral-pion production.

The model displays chiral symmetry, gauge invariance, and crossing symmetry as well as a consistent treatment of the spin-3/2 interaction which overcomes pathologies present in former analysis [21]. Under this approach for spin-3/2 interactions the (spin-3/2 resonance)-nucleon-pion and the (spin 3/2 resonance)-nucleon-photon vertices have to fulfill the condition $q_\alpha \mathcal{O}^{\alpha\cdots} = 0$ where q is the four-momentum of the spin-3/2 particle, α the vertex index which couples to the spin-3/2 field, and the dots stand for other possible indices. In particular, for the $\Delta(1232)$, the simplest interacting π-N-$\Delta(1232)$ Lagrangian is [21]

$$\mathscr{L}_{\pi N\Delta} = -\frac{h}{f_\pi M_\Delta}\bar{N}\epsilon_{\mu\nu\lambda\beta}\gamma^\beta\gamma^5\left(\partial^\mu\Delta_j^\nu\right)\left(\partial^\lambda\pi_j\right) + \text{H.c.}, \qquad (13)$$

where H.c. stands for hermitian conjugate, h is the strong coupling constant, $f_\pi = 92.3$ MeV is the leptonic decay constant of the pion, M_Δ the mass of the $\Delta(1232)$, and Δ_j^ν the $\Delta(1232)$ field. The γ-N-$\Delta(1232)$ interaction can be written [22]

$$\mathscr{L}_{\gamma N\Delta} = \frac{3e}{2M_N M_+}\bar{N}\left[\frac{ig_1}{2}\tilde{F}_{\mu\nu} + g_2\gamma^5 F_{\mu\nu}\right]\left(\partial^\mu\Delta_3^\nu\right) + \text{H.c.}, \qquad (14)$$

where g_1 and g_2 are the electromagnetic coupling constants, $M_+ = M_N + M_\Delta$, and $\tilde{F}_{\mu\nu} = \epsilon_{\mu\nu\alpha\beta}F^{\alpha\beta}$.

The dressing of the resonances is considered by means of a phenomenological width which contributes to both s and u channels and takes into account decays into one π, one η, and two π. The energy dependence of the width is chosen phenomenologically as

$$\Gamma(s,u) = \sum_{j=\pi,\pi\pi,\eta}\Gamma_j X_j(s,u), \qquad (15)$$

where s and u are the Mandelstam variables and

$$X_j(s,u) \equiv X_j(s) + X_j(u) - X_j(s)X_j(u), \qquad (16)$$

with $X_j(l)$ given by

$$X_j(l)=2\frac{\left(\frac{|\vec{k}_j|}{|\vec{k}_{j0}|}\right)^{2L+1}}{1+\left(\frac{|\vec{k}_j|}{|\vec{k}_{j0}|}\right)^{2L+3}}\Theta\left(l-\left(M_N+m_j\right)^2\right), \tag{17}$$

where L is the angular momentum of the resonance, Θ is the Heaviside step function, and

$$|\vec{k}_j|=\sqrt{\left(l-M_N^2-m_j^2\right)^2-4m_j^2M_N^2}\Big/\left(2\sqrt{l}\right), \tag{18}$$

with $m_{\pi\pi}\equiv 2m_\pi$ and $|\vec{k}_{j0}|=|\vec{k}_j|$ when $l=M^{*2}$ (M^* stands for the mass of the resonance).

This parameterization has been built in order to fulfill the following conditions

(i) $\Gamma=\Gamma_0$ at $\sqrt{s}=M^*$;

(ii) $\Gamma\to 0$ when $|\vec{k}_j|\to 0$;

(iii) a correct angular momentum barrier at threshold $|\vec{k}_j|^{2L+1}$;

(iv) crossing symmetry.

For the resonance-pion-nucleon vertex, the form factor $\sqrt{X_\pi(s,u)}$ has to be used for consistency with the width employed.

In order to regularize the high energy behavior of the model a crossing symmetric and gauge invariant form factor is included for Born and vector meson exchange terms,

$$\hat{F}_B(s,u,t)=F(s)+F(u)+G(t)-F(s)F(u)-F(s)G(t)-F(u)G(t)+F(s)F(u)G(t), \tag{19}$$

where

$$F(l)=\left[1+\left(l-M_N^2\right)^2/\Lambda^4\right]^{-1}, \qquad l=s,u, \tag{20}$$

$$G(t)=\left[1+\left(t-m_\pi^2\right)^2/\Lambda^4\right]^{-1}. \tag{21}$$

For vector mesons $\hat{F}_V(t)=G(t)$ is adopted with the change $m_\pi\to m_V$. The cut-off $\Lambda=1.050$ GeV in the case of dressed pion production amplitudes, whereas $\Lambda=0.951$ GeV in the case of bare ones.

In the pion photoproduction model from free nucleons [3] it was assumed that FSI factorize and can be included through the distortion of the πN final state wave function (pion-nucleon rescattering). πN-FSI was included by adding a phase δ_{FSI} to the electromagnetic multipoles. This phase is set so that the total phase of the multipole matches the total phase of the energy dependent solution of SAID [23]. In this way it was possible to isolate the contribution of the bare diagrams to the physical observables. The parameters of the resonances were extracted fitting the data to the electromagnetic multipoles from the energy independent solution of SAID [23] applying modern optimization techniques based upon a genetic algorithm combined with gradient based routines [24] which provides reliable values for the parameters of the nucleon resonances. Once the parameters, including phase shifts, are fitted to data we can distinguish between bare and dressed photo-pion production amplitudes on the nucleon. In what follows we call bare amplitudes to the ones provided by our model using the fitted values for all the parameters except those of the phase shifts which are set to zero.

In order to examine the various observables for pion photoproduction on the free nucleon we provide in Fig. 4 results for the polarized nucleon-target asymmetry T as a function of pion angle at photon lab-energy of $E_\gamma = 300$ MeV. Results for the various pion photoproduction channels from the free nucleon are given using the ELA model [3]. We see that the agreement of the results using the ELA model (solid curves) in comparison with the data from SAID [23] is good and give a clear indication that the ELA model [3] can be applied directly to calculate the electromagnetic photoproduction of pions from the deuteron.

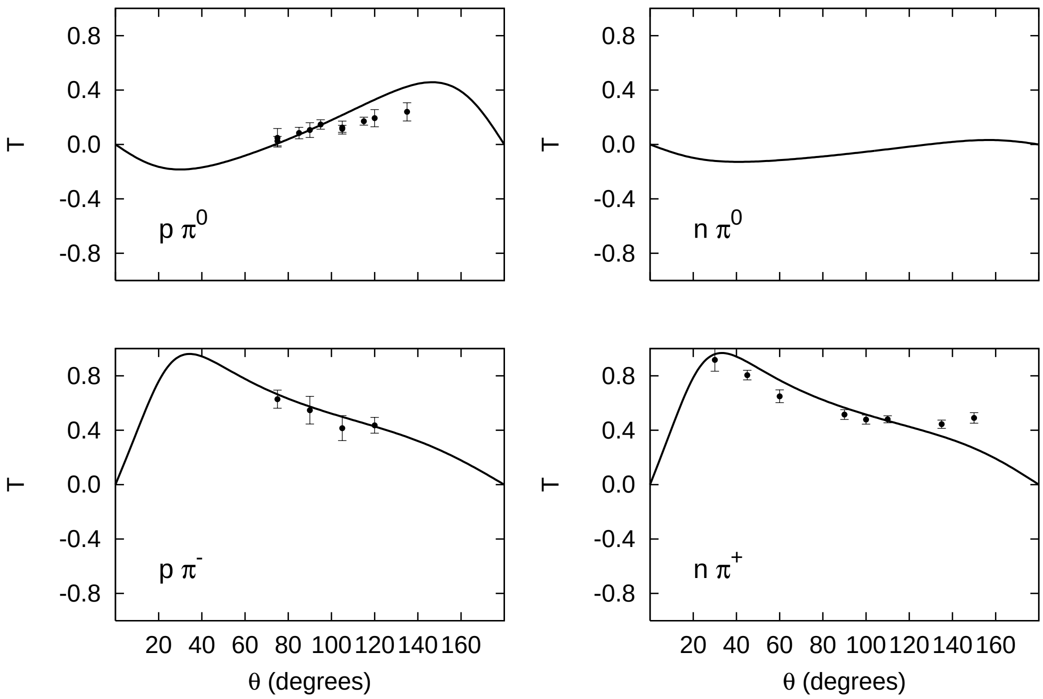

Figure 4: Polarized nucleon-target asymmetry T as a function of pion angle for the four different channels of pion photoproduction from free nucleons calculated at $E_\gamma = 300$ MeV. Solid curve stands for the calculation using the effective Lagrangian approach (ELA) [3]. Data are taken from SAID [23].

3 Results and discussion

In this section we explore the dependence of the results for the observables in the $\gamma d \to \pi^0 d$ reaction on the input elementary pion photoproduction operator. We show results for the unpolarized total and differential cross sections in the energy region from π-threshold up to 1 GeV in comparison with the available experimental data, using as elementary reaction amplitudes the ones provided by the ELA model from Ref. [3] and those obtained using MAID model [25]. For the deuteron wave function, we use for both the initial and final deuteron states the realistic high-precision CD-Bonn potential model [14].

We would like to explain carefully what we call IA and how we compute it. Our IA calculation does not employ directly the amplitudes that fit the data on electromagnetic multipoles for the $\gamma N \to \pi N$ process. This is due to the fact that πN-rescattering is unavoidably included in the amplitude in these fits to data. We call IA to the bare contribution to the observables. Therefore, if we wish to calculate the contribution coming from the pure IA, the bare IA contribution to the amplitude has to be extracted from the analysis of the $\gamma N \to \pi N$, where the final state interaction has to be removed. This was done in Ref. [3]. We name IA* to the calculations where the πN-rescattering is included in the elementary pion photoproduction reaction on the free nucleon.

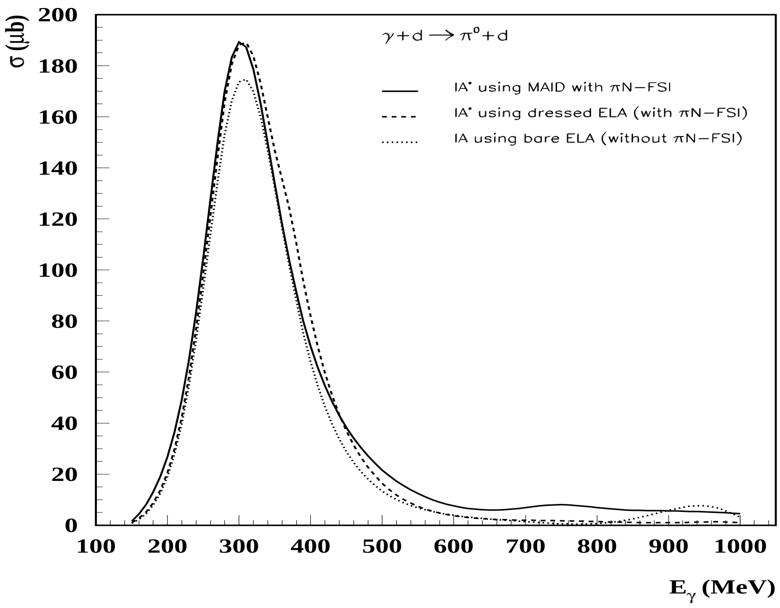

Figure 5: Total cross section for coherent pion photoproduction on the deuteron $\gamma d \to \pi^0 d$ as a function of photon lab-energy. The solid curve shows the results of IA* using the MAID model [25]. The dashed (dotted) curve shows the results of IA* (IA) using the dressed (bare) electromagnetic multipoles of ELA model [3].

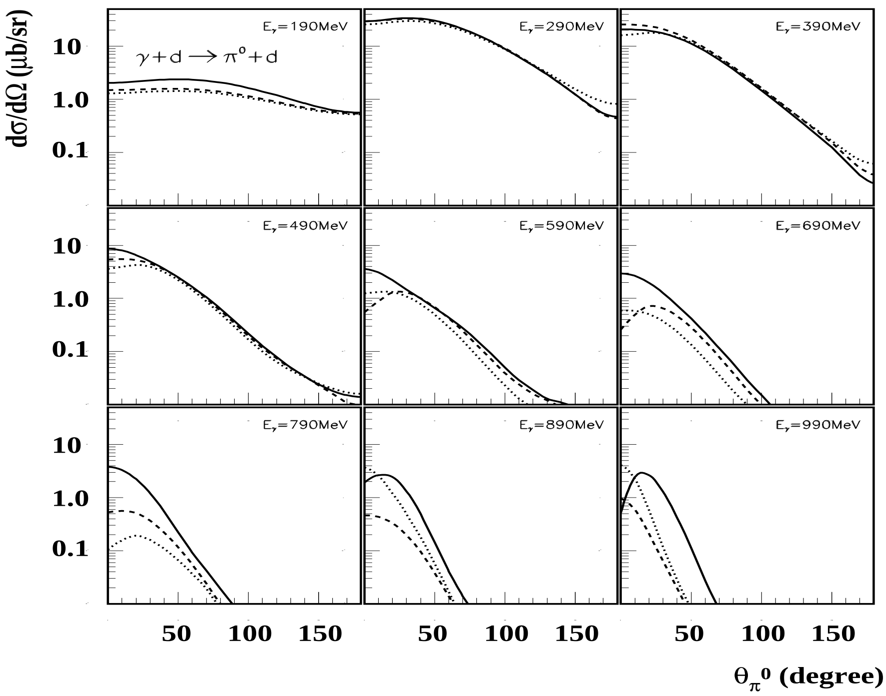

Figure 6: Differential cross sections for coherent π^0-photoproduction on the deuteron as a function of pion angle in the c.m. frame at nine different values of photon energy in the lab. frame. The meaning of curves is explained in the caption of Fig. 5.

The first comparison (Fig. 5) shows the sensitivity of the results for total cross section on the elementary pion photoproduction operator using the CD-Bonn potential [14] for the deuteron wave function in the energy region from π-threshold up to 1 GeV. The solid curve shows the results of IA* using the MAID model [25], whereas the dashed (dotted) curve shows the results of IA* (IA) using the dressed (bare) electromagnetic multipoles of ELA model [3]. As already mentioned, IA* denotes the deuteron calculation when the πN-rescattering is included in the elementary reaction.

We find that the total cross section presents qualitative a similar behavior for different elementary operators. One sees that the total cross section has a peak at photon lab-energy of about 350 MeV due to the dominant excitation of the M_{1+} multipole on the free nucleon. The maximum of this peak is greater in IA* than in IA and therefore careful must be taken when one uses elementary reactions in nuclear applications. It is also clear that the computations with different elementary amplitudes are quite different. For example, at the peak position we obtain larger values using MAID and ELA with πN-FSI than using ELA without πN-FSI. Similarly, a bump-like structure is observed at photon lab-energy of about 750 MeV using the MAID model, whereas it is observed at higher energies when one uses the ELA model. These discrepancies show up the differences among elementary operators which are obvious at photon lab-energies above 500 MeV. This means that the total cross section is sensitive to the choice of the elementary amplitude, especially at high photon lab-energies. The difference between the dashed (dressed ELA) and dotted (bare ELA) curves shows the effect of πN-rescattering in the elementary $\gamma N \to \pi N$ amplitude, which is also found to be important.

Fig. 6 shows our results for differential cross section as a function of pion angle in the c.m. frame at various values of photon lab-energy. We show the sensitivity of the results for differential cross section on the elementary pion photoproduction operator using the CD-Bonn potential [14] for the deuteron wave function. We find that the differential cross section presents qualitative similar behavior for different elementary operators. It is clear that the computations with different elementary amplitudes are quite different, in particular at forward pion angles and at high photon energies. At backward angles, one sees that the differential cross section is small in comparison to the results at forward angles. It is seen that the differential cross section vanishes at energies above 500 MeV at backward angles. As in the case of total cross section, obvious differences are shown when one uses the MAID model [25] (solid curve) and ELA model [3] (dotted and dashed curves). These discrepancies show up the differences among elementary operators which are very clear at forward pion angles for

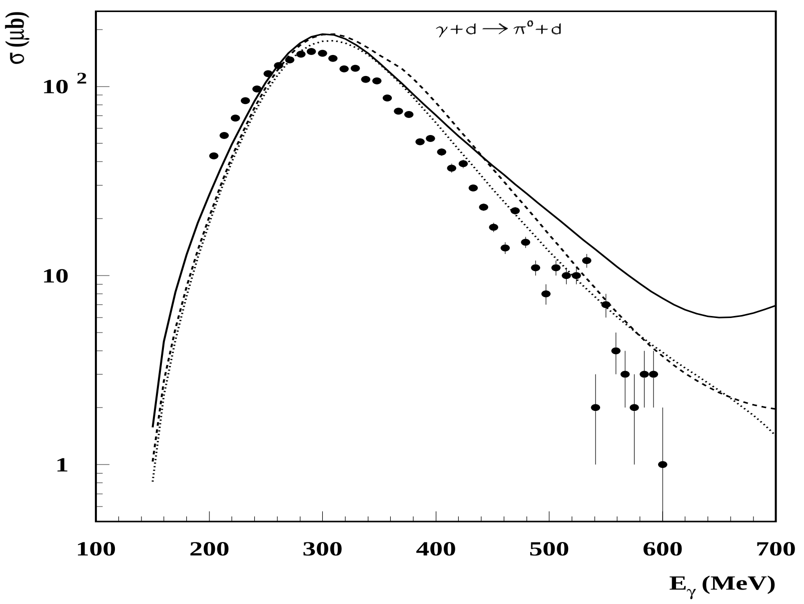

Figure 7: Total cross section for coherent π^0-photoproduction on the deuteron, using the logarithmic scale, as a function of photon lab-energy in comparison with experimental data. The meaning of curves is explained in the caption of Fig. 5. The data points are taken from TAPS [26].

photon lab-energies above 500 MeV.

Now, we compare our predictions for unpolarized total and differential cross sections of the $\gamma d \to \pi^0 d$ reaction with the available experimental data. Fig. 7 shows the results for the total cross section as a function of photon energy in the laboratory frame in comparison with the experimental data from TAPS [26]. We compare results using as elementary reaction amplitudes, the ones provided by the ELA model of Ref. [3] and those obtained using MAID model [25]. For the deuteron wave function we use the realistic high-precision CD-Bonn potential model [14]. The solid curve in Fig. 7 shows the results using the MAID model [25], the dashed (dotted) curve shows the results using the dressed (bare) electromagnetic multipoles of the ELA model [3].

One readily observed, that the dotted curve which represents the results using the bare electromagnetic multipoles of the ELA model [3] is the nearest one to the experimental data, especially after the peak position. However, the agreement between the results using the MAID model [25] and the experimental data from TAPS [26] is quantitatively not good. One also sees, that none of the models is able to describe the right position of the peak, as well as the behavior of the data points after the peak. In principle, one can speculate that our results using the bare electromagnetic multipoles of the ELA model [3] agrees with the slope at high photon lab-energy, but the results using the MAID model are not. This means in particular that the results are strongly dependent on the pion production on the free nucleon and, therefore, one must look more in deep for the reasons in the different results.

As next, we compare our results for the unpolarized differential cross section of the $\gamma d \to \pi^0 d$ reaction as a function of the emission pion angle at four various values of photon lab-energy with the experimental data from TAPS [27] as shown in Fig. 8. As in the case of total cross section, we compare results using as elementary reaction amplitude, the ones provided by the ELA model of Ref. [3] and those obtained using MAID model [25]. For the deuteron wave function we also use the realistic high-precision CD-Bonn potential model [14].

At energies less than the $\Delta(1232)$-resonance region, one notes that the agreement between our results using different elementary operator is not satisfactory. The reason for this may be due to the neglecting πN-rescattering in the intermediate state which is found to be important [12]. On the contrary, we obtained a qualitatively reasonable agreement between our results and the experimental data from TAPS [27] at energies around the Δ-region. At forward pion angles and high energy, an overestimation of our results using various elementary amplitudes is found. The solid curve which represents the results using the MAID model [25] is the nearest one to the experimental data even at forward pion angle and small energy. Discrepancies between the results using different elementary amplitudes are found at extreme forward pion angles, whereas at backward pion angles discrepancies are observed at small energies. An experimental check of these predictions at extreme forward pion angles is needed.

From the preceding discussion it is apparent that the choice of the elementary operator has a visible effect on cross sections. Summarizing, we can say that the MAID model [25] provides different predictions for cross sections than the ELA model [3] and that these cross sections provide excellent observables to test different pion production operators.

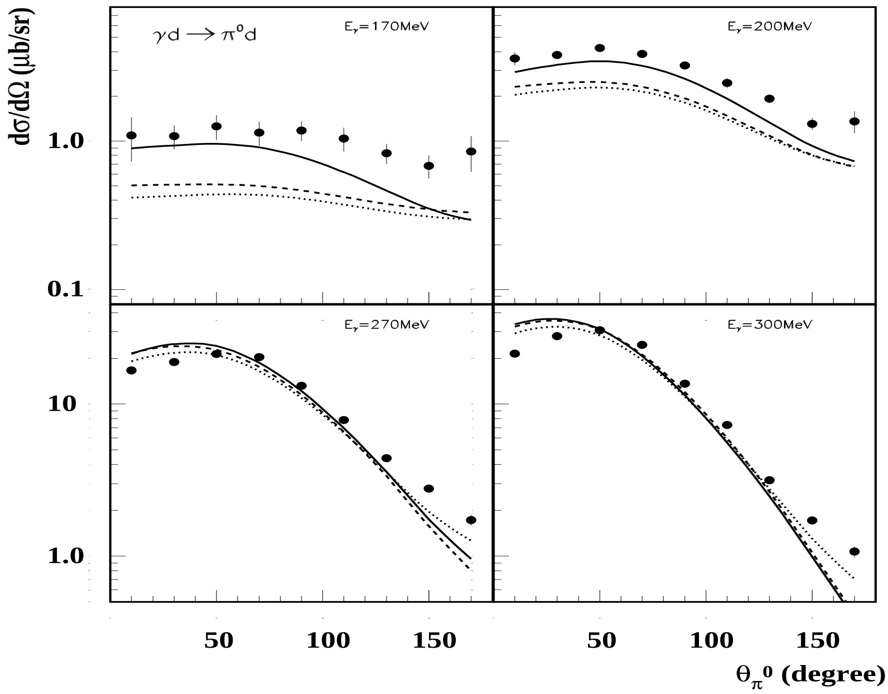

Figure 8: Differential cross sections for coherent π^0-photoproduction on the deuteron, using the logarithmic scale, as a function of pion angle in the center-of-mass frame at four different values of photon lab-energy. The meaning of curves is explained in the caption of Fig. 5. The data points are taken from TAPS [27].

4 Conclusions

The main topic of this paper was the investigation of the coherent π^0-photoproduction reaction on the deuteron. Results for total and differential cross sections are presented, in the energy region from π-threshold up to photon lab-energy of 1 GeV, and compared with the available experimental data. For the elementary pion photoproduction operator, a realistic effective Lagrangian approach has been used which displays chiral symmetry, gauge invariance, and crossing symmetry, as well as a consistent treatment of the spin-3/2 interaction. For the deuteron wave function, the realistic high-precision CD-Bonn potential model [14] was used. The sensitivity of the results to the elementary pion photoproduction operator on the free nucleon has also been investigated.

Within our model, we have found that the total and differential cross sections are sensitive to the choice of the elementary operator. In many cases, the deviation among results obtained using different elementary operators is very large. In view of these results, we conclude that the process $d(\gamma,\pi^0)d$ can serve as a filter for different elementary operators since their predictions provide very different values for observables.

Finally, we would like to point out that future improvements of the present model can be achieved by including pion rescattering and two-body effects. In addition, polarization observables constitute more stringent tests for theoretical models due to their sensitivity to small amplitudes. At this point, measurements on the deuteron spin asymmetries will certainly provide us with an important observable to test our knowledge of the pion photoproduction on the free neutron process.

Acknowledgments. The work of E.M. Darwish was supported by the Deanship of Scientific Research of the Taibah University, Saudi Arabia under project No. 430/403. The work of N. Akopov was supported by the ISTC grant under project A-1606. M. El-Zohry would like to thank Prof. V. Tsakanov for many useful discussion and support.

References

[1] B. Krusche and S. Schadmand, Prog. Part. Nucl. Phys. 51, (2003) 399.

[2] E. M. Darwish, C. Fernández-Ramírez, E. Moya de Guerra, and J. M. Udías, Phys. Rev. C 76 (2007) 044005; E. M. Darwish, C. Fernández-Ramírez, E. Moya de Guerra, and J. M. Udías, AIP Conf. Proc. 1006 (2008) 165.

[3] C. Fernández-Ramírez, E. Moya de Guerra, and J.M. Udías, Ann. Phys. (N.Y.) 321 (2006) 1408; C. Fernández-Ramírez, Ph. D. Dissertation(Universidad Complutense de Madrid, Spain, 2006); C. Fernández-Ramírez, E. Moya de Guerra, and J. M. Udías, Phys. Lett. B 660 (2008) 188.

[4] J. H. Koch and R. M. Woloshyn, Phys. Rev. C 16 (1977) 1968.

[5] P. Bosted and J. M. Laget, Nucl. Phys. A 296 (1978) 413; J.M. Laget, Phys. Rep. 69 (1981) 1.

[6] P. Wilhelm and H. Arenhövel, Few-Body Syst. Suppl. 7 (1994) 235; P. Wilhelm and H. Arenhövel, Nucl. Phys. A 593 (1995) 435.

[7] H. Garcilazo and E. M. de Guerra, Phys. Rev. C 52 (1995) 49.

[8] F. Blaazer, B. L. G. Bakker, and H. J. Boersma, Nucl. Phys. A 590 (1995) 750; F. Blaazer, Ph. D. Dissertation (Free University of Amsterdam, Amsterdam, 1995).

[9] A. K. Kerman, H. McManus, and R. M. Thaler, Ann. Phys. (N.Y.) 8 (1959) 551.

[10] S. S. Kamalov, L. Tiator, and C. Bennhold, Nucl. Phys. A 547 (1992) 559; S. S. Kamalov, L. Tiator, and C. Bennhold, Few-Body Syst. 10 (1991) 143; S. S. Kamalov, L. Tiator, and C. Bennhold, Phys. Rev. C 55 (1997) 98.

[11] A. E. Kudryavtsev , V. E. Tarasov, I. I. Strakovsky, *et al.*, Phys. Rev. C 71 (2005) 035202.

[12] A. Fix, Eur. Phys. J. A 26 (2005) 293.

[13] E. M. Darwish and M. Y. Hussein, Proceedings of the 4th Annual Meeting of the Saudi Physical Society (King Abdulaziz City for Science and Technology, Riyadh, 2008); Appl. Math. & Inf. Sci. 3 (2009) 321.

[14] R. Machleidt, F. Sammarruca, and Y. Song, Phys. Rev. C 53 (1996) R1483; R. Machleidt, Phys. Rev. C 63 (2001) 024001.

[15] J. D. Bjorken and S. D. Drell, Relativistic Quantum Mechanics (McGraw-Hill, New York, 1964).

[16] C. Fernández-Ramírez, E. Moya de Guerra, and J. M. Udías, Phys. Rev. C 73 (2006) 042201(R); C. Fernández-Ramírez, E. Moya de Guerra, and J. M. Udías, Eur. Phys. J. A 31 (2007) 572.

[17] Review of Particle Physics, W. M. Yao, *et al.*, J. Phys. G 33 (2006) 1.

[18] G. Blanpied *et al.*, Phys. Rev. C 64 (2001) 025203; J. Ahrens *et al.*, Eur. Phys. J. A bf 21 (2004) 323; S. Stave *et al.*, Eur. Phys. J. A 30, (2006), 471.

[19] C. Alexandrou, Ph. de Forcrand, H. Neff, *et al.*, Phys. Rev. Lett. 94 (2005) 021601.
[20] C. Fernández-Ramírez, E. Moya de Guerra, and J. M. Udías, Phys. Lett. B 651 (2007) 369.
[21] V. Pascalutsa, Phys. Rev. D 58 (1998) 096002; V. Pascalutsa and R. Timmermans, Phys. Rev. C 60 (1999) 042201.
[22] V. Pascalutsa and D. R. Phillips, Phys. Rev. C 67 (2003) 055202.
[23] R. A. Arndt and D. Roper, The Scattering Analysis Interactive Dial-In Program (SAID), SAID database, `http://gwdac.phys.gwu.edu`. For further references see, for example, R. A. Arndt, I. I. Strakovsky and R. L. Workman, Phys. Rev. C 53 (1996) 430; R. A. Arndt, R. L. Workman, Z. Li and L.D. Roper, Phys. Rev. C 42 (1990) 1853; R. A. Arndt, W. J. Briscoe, I. I. Strakovsky, and R. L. Workman, Phys. Rev. C 66 (2002) 055213.
[24] D. G. Ireland, S. Janssen, and J. Ryckebusch, Nucl. Phys. A 740 (2004) 147; C. Fernández-Ramírez, E. Moya de Guerra, A. Udías, and J. M. Udías, Phys. Rev. C 77 (2008) 065212.
[25] O. Hanstein, D. Drechsel, and L. Tiator, Nucl. Phys. A 632 (1998) 561; D. Drechsel, O. Hanstein, S. Kamalov, and L. Tiator, Nucl. Phys. A 645 (1999) 145; D. Drechsel, S. Kamalov, and L. Tiator, Eur. Phys. J. A 34 (2007) 69; *MAID Program*, Institut für Kernphysik, Johannes Gutenberg-Universität, Mainz, Germany. `http://www.kph.uni-mainz.de/de/MAID/`.
[26] B. Krusche, J. Ahrens, R. Beck, *et al.*, Eur. Phys. J. A 6 (1999) 309.
[27] U. Siodlaczek, Ph. D. Dissertation (Tübingen University, Germany, 2000).